CrossMark

ORIGINAL PAPER

Punctuated evolution of viscid silk in spider orb webs supported by mechanical behavior of wet cribellate silk

Dakota Piorkowski[1,2] · Todd A. Blackledge[1,3]

Abstract The origin of viscid capture silk in orb webs, from cribellate silk-spinning ancestors, is a key innovation correlated with significant diversification of web-building spiders. Ancestral cribellate silk consists of dry nanofibrils surrounding a stiff, axial fiber that adheres to prey through van der Waals interactions, capillary forces, and physical entanglement. In contrast, viscid silk uses chemically adhesive aqueous glue coated onto a highly compliant and extensible flagelliform core silk. The extensibility of the flagelliform fiber accounts for half of the total work of adhesion for viscid silk and is enabled by water in the aqueous coating. Recent cDNA libraries revealed the expression of flagelliform silk proteins in cribellate orb-weaving spiders. We hypothesized that the presence of flagelliform proteins in cribellate silk could have allowed for a gradual shift in mechanical performance of cribellate axial silk, whose effect was masked by the dry nature of its adhesive. We measured supercontraction and mechanical performance of cribellate axial silk, in wet and dry states, for two species of cribellate orb web-weaving spiders to see if water enabled flagelliform silk-like performance. We found that compliance and extensibility of wet cribellate silk increased compared to dry state as expected. However, when compared to other silk types, the response to water was more

similar to other web silks, like major and minor ampullate silk, than to viscid silk. These findings support the punctuated evolution of viscid silk mechanical performance.

Keywords Biomaterial · Spider · Silk · Cribellate · Orb web · Tensile properties

✉ Todd A. Blackledge
   blackledge@uakron.edu

[1] Department of Biology, The University of Akron, Akron, OH 44325-3908, USA

[2] Present address: Department of Life Science, Tunghai University, Taichung 40704, Taiwan

[3] Department of Biology, Integrated Bioscience Program, The University of Akron, Akron, OH 44325, USA

Introduction

Spider orb webs intercept flying insects using a combination of strong supporting threads and adhesive capture silk (Blackledge et al. 2011; Foelix 2011). Adhesive cribellate silk arose early in the evolution of "true spiders" (Araneomorphae) and many architectures of cribellate webs appeared by 223–330 million years ago (Garrison et al. 2016). However, subsequent spider evolution is marked by a persistent loss of webs in a variety of clades, including the megadiverse RTA clade of mostly cursorial hunting spiders (Bond et al. 2014; Fernandez et al. 2014; Garrison et al. 2016). The frequent loss of cribellate silk is hypothesized to be due in part to the high costs of producing cribellate silk (Eberhard 1990; Coddington and Levi 1991; Blackledge et al. 2009a, b). For instance, the puffy nanofibrils must be tediously combed out of the spider's cribellum and laid along an axial thread (Zschokke and Vollrath 1995; Opell 1997; Joel et al. 2015). The emergence of orb webs utilizing novel viscid capture silk, likely in the Jurassic, is linked to the largest diversification of web-building spiders and the origins of many new types of web architectures (Coddington and Levi 1991; Bond and Opell 1998; Opell and Bond 2001; Blackledge et al. 2009a, b). Viscid silk requires less time to produce than cribellate silk (Zschokke and Vollrath 1995 and more efficiently recruits adhesion across surfaces than cribellate silk (Opell and Schwend 2009). Viscid silk-spinning spiders clearly arose

from a cribellate ancestor (Eberhard 1990; Coddington and Levi 1991; Blackledge et al. 2009a, b; Garrison et al. 2016). But, how that transition between two such divergent and complex phenotypes occurred is unknown. Did viscid silk arise through a gradual transition from cribellate silk, or as a punctuated emergence of a functionally integrated set of traits?

The dramatic differences in spider capture silks once led researchers to argue that cribellate and ecribellate orb webs represented a striking case of convergent evolution in web-building behaviors (Kullmann 1972; Eberhard 1982). However, similar leg movement patterns during web construction (Coddington 1982, 1990; Eberhard 1982, 1990), similar environmental cues guiding orb web construction behaviors, (Eberhard and Barrantes 2015), and similar morphologies of the flagelliform and pseudoflagelliform glands (Griswold et al. 1999; Griswold et al. 2005) argued for a single origin of orb-weaving behaviors followed by a transition from cribellate to viscid capture threads. Early molecular phylogenetic studies found additional support for the monophyly of orb web spider lineages (Blackledge et al. 2009a, b; Dimitrov et al. 2011). Finally, cDNA libraries also found evidence for the expression of flagelliform silk genes in the silk glands of cribellate orb-weaving spiders (Garb et al. 2006). Together, these studies suggest that orb-weaving first evolved in a cribellate spider with a subsequent transition in capture silk production to viscid threads occurring in an orb-weaving taxon.

However, recent phylogenomic studies suggest a more ancient origin of orb-weaving behaviors (Bond et al. 2014; Fernandez et al. 2014), with viscid silk orb-weaving spiders sister to a group of spiders with much more diverse web-spinning behaviors, but still ancestrally cribellate (Garrison et al. 2016). Therefore, to understand the origin of viscid silk, it is useful to think of web architecture and capture silk type as separate traits. Regardless of the web-spinning behaviors of the ancestor from which viscid orb-weaving spiders evolved, the transition from cribellate capture silk to viscid capture silk is supported by all of these different investigations (Coddington 1986; Griswold et al. 1999; Opell and Bond 2000).

The divergent morphology and properties of viscid and cribellate silk (Köhler and Vollrath 1995; Blackledge and Hayashi 2006a) present two complex character systems whose function is derived from a set of interdependent parts that are not easily combined into an intermediate silk type. This argues for a rapid transition from cribellate to viscid silk. However, a gradual transition in adhesive silk performance has also been hypothesized (Opell and Bond 2000; Opell et al. 2011b) and is supported by experimentally produced cribellate-viscid silk hybrid threads that show higher stickiness and adhesive efficiency than either silk type alone (Opell et al. 2011a, b). They suggest that viscid silk secretions

might have evolved initially to allow young spiders to produce adhesive threads before their spinnerets were capable of producing cribellate silk. Then selection might have co-opted the use of the viscid secretions so that they were added to axial threads before the addition of the cribellate fibrils, providing hygroscopicity and improving adhesion, before the glands producing cribellate silk were eventually lost (Opell et al. 2011a, b). Here, we focus on the transition in the mechanical performance of the underlying axial fibers, which play a key role in adhesion and differ markedly between the two silk types.

Dry cribellate silk (Fig. 1) operates as a composite structure with a strong, but stiff, axial fiber supporting ultra-fine cribellate fibrils that adhere prey (Opell 1994; Hawthorn and Opell 2002, 2003; Blackledge and Hayashi 2006a). Cribellate axial fiber tensile behavior is, qualitatively, similar to that of major ampullate silk demonstrating an initial elasticity followed by yielding and moderate compliance, and then finally an increase in stiffness before failure (Blackledge and Hayashi 2006a). Cribellate fibrils adhere through van der Waals and hygroscopic forces (Hawthorn and Opell 2003) and capillary interactions with the waxes on arthropod cuticles (Bott et al. 2017). Cribellate silk must remain dry to generate useful adhesion because wetting clumps the fibrils and makes substrate attachment less effective (Elettro et al. 2015).

In contrast, viscid capture silk must remain wet because it becomes less adhesive and mechanically underperforms when dry (Vollrath and Edmonds 1989; Opell et al. 2011a; Perea et al. 2013; Amarpuri et al. 2015). Viscid silk (Fig. 1) is also composed of a highly extensible flagelliform silk axial fiber coated in aqueous, aggregate glue (Peters 1987; Vollrath and Edmonds 1989; Blackledge and Hayashi 2006b; Opell and Hendricks 2007). However, when wetted by the surrounding glue, flagelliform silk becomes rubber-like, able to extend five to ten times its original length while recovering even after stretching ~100% (Gosline et al. 1984; Vollrath and Edmonds 1989; Swanson et al. 2007). This extensibility is
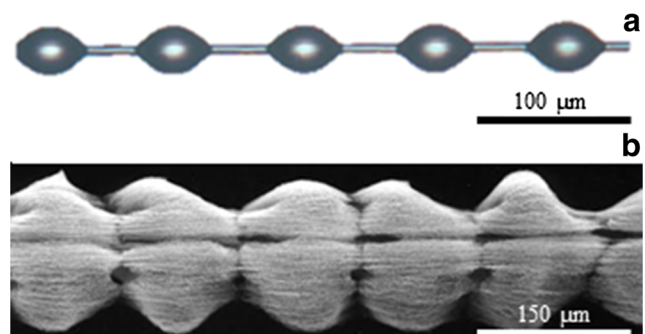

Fig. 1 **a** Flagelliform silk coated in droplets of sticky, aqueous glue make up viscid capture threads while **b** cribellate silk is composed of an axial core fiber surrounded by thousands of dry-adhesive cribellar nanofibrils. Panel **a** reprinted from Opell (1999) with permission from B. Opell and panel **b** reprinted from Blackledge et al. (2009a) with permission

important because the flagelliform silk fiber performs about half the work of adhesion as force is summed and transferred from glue droplets attached to the substrate in what is known as the "suspension bridge" mechanism (Opell and Hendricks 2007; Sahni et al. 2010).

The high extensibility and compliance of the flagelliform fiber are generated through an interaction between the composing protein molecules and water (Vollrath and Edmonds 1989; Hayashi and Lewis 1998). Highly repeated glycine-proline-glycine-XX (GPGXX) amino acid motifs in the flagelliform silk proteins (Flag spidroins) fold the flagelliform protein backbone into spring-like molecular configurations (Hayashi and Lewis 1998; Hayashi and Lewis 2000), while water interacts with these "nanosprings" by disrupting inter-molecular H-bonding (Eles and Michal 2004; Savage and Gosline 2008). This allows fibers to reversibly contract to higher entropy states, a process also known as supercontraction (Termonia 1994; Yang et al. 2000; Eles and Michal 2004), which confers macroscopic properties of low stiffness and high extensibility.

The GPGXX motif occurs in other spidroins, particularly major ampullate spidroin 2 (MASP2), which is one of two main protein constituents of dry dragline silk. While GPGXX is not repeated nearly as often in MASP2 compared to flagelliform silk, variation in the expression of the protein is thought to explain differences in proline concentration and hence determine some of the variation in major ampullate silk performance both within (Marhabaie et al. 2014) and among species (Liu et al. 2008; Boutry and Blackledge 2010). However, major ampullate silk is ~3 orders of magnitude stiffer and only ~10% as extensible as flagelliform silk (Blackledge and Hayashi 2006b). Its performance is also substantially less water-dependent compared to flagelliform silk (Guinea et al. 2010; Perea et al. 2013). Thus, comparison of the mechanical performance of silks, especially between wet and dry states, can give insight into the degree to which GPGXX motifs are present in the spidroins.

Flagelliform spidroins (silk proteins) were once thought to be unique to ecribellate orb-weaving spiders based upon cDNA libraries produced from the silk glands of araneoid orb spiders compared to non-orb-weaving taxa (Gatesy et al. 2001). However, more recent cDNA libraries generated from silk gland tissue of cribellate orb web spiders identified the expression of flagelliform-like proteins in silk glands of cribellate orb web spiders (Garb et al. 2006). While Garb et al. did not directly quantify proteins in the silk, the potential expression of flagelliform silk proteins in cribellate spiders suggests an intriguing hypothesis that some of the molecular architecture giving rise to viscid silk's unique tensile mechanics could have evolved earlier than the viscid silk itself.

If there is expression of flagelliform silk proteins in cribellate orb-weaving spiders (Garb et al. 2006), the effects of the –GPGGX– amino acid motif on silk structure would be masked by the dry nature of the cribellate composite thread. Thus, the high extensibility of flagelliform silk could be an exaptation (Gould and Vrba 1982), a beneficial trait resulting from an existing molecular structure in the pseudoflagelliform axial threads of cribellate silk but providing a functional advantage only after the evolution of aqueous glue. In this study, we test the prediction that cribellate axial threads will perform mechanically like viscid axial threads when plasticized by water.

Materials and methods

Spiders and silk

Cribellate silk was collected from webs of two species of orb-weaving spiders. *Uloborus plumipes* were collected from University of Ljubljana, Slovenia and allowed to construct orb webs in cylindrical wire mesh and screen containers (20-cm diameter × 10-cm height). Captive spiders were fed fruit flies and misted with water every 1–3 days. After 7 days of acclimation, silk was collected from freshly constructed webs. Whole webs of *Hyptiotes cavatus* were collected in the field from Bath Nature Preserve, Bath, Ohio, USA. *Hyptiotes* spin a reduced orb web that was collected intact on cardboard frames lined with double-sided sticky tape to preserve original web tension. Silk threads were collected from both types of webs using c-shaped cardboard frames across gaps 10 to 15 mm in length as described in Blackledge and Hayashi (2006a). Threads were secured using Elmer's School Glue.

We considered untreated cribellate silk collected from naturally spun webs in natural and laboratory conditions to be in a "native," dry state as silk was neither forcibly drawn (Work 1976; Pérez-Rigueiro et al. 2005) nor coaxed out of the spiders through behavioral manipulation (Boutry et al. 2011). We did not remove the cribellate fibrils to prevent damage to the axial thread; however, we assume minimal mechanical contribution of the cribellate fibrils prior to the breaking of the axial fiber as previously described by Blackledge and Hayashi (2006a). We did not report mechanical performance of cribellate fibrils post-axial thread breakage (but *See* Blackledge and Hayashi 2006a).

Silk diameter measurement and mechanical testing

Polarized light microscopy was used to determine diameters of individual axial silk threads prior to mechanical testing (Blackledge et al. 2005). Cross-sectional areas for double-stranded axial threads were calculated as the sum of cross-sectional areas for each fiber. Diameters of cribellate fibrils surrounding the axial thread were not measured because they contribute minimally to resisting loading compared to the thicker axial threads.

A Nano Bionix® tensile tester (MTS) was used to generate load-extension data of cribellate silk threads pulled to breaking with an extension rate of 1.5% strain s^{-1} (Blackledge and Hayashi 2006a, b). Dry treatment samples were tested at ambient humidity (~30% RH). Wet treatment samples were mounted within an environmental chamber at ambient humidity, and relative humidity was brought to >90% over 2 min to ensure silk samples were saturated directly prior to testing as described in Boutry and Blackledge (2010). Gage length and diameter were recalculated for samples after wetting to account for possible effects of supercontraction. Assuming constant volume of the silk fiber during supercontraction (Guinea et al. 2006), $A_1 L_1 = A_2 L_2$, where A refers to the fiber cross-sectional area, L refers to the fiber gage length, subscript 1 indicates the original state of the fiber, and subscript 2 indicates the fiber after wetting. However, we find negligible supercontraction from wetting (See below "Materials and methods" and "Results") and therefore minimal change in diameter and gage length.

True stress was calculated as, $\sigma_t = F / A$, where F is the force applied and A is the instantaneous cross-sectional area assuming constant volume. True strain was calculated as, $\varepsilon_t = \ln(L / L_0)$, where L is the instantaneous gage length and L_0 is initial gage length. We determined (i) tensile strength as true stress at breaking, (ii) extensibility as true strain at breaking, (iii) initial resistance to deformation as Young's modulus, and (iv) work to break per volume or toughness. Young's modulus was calculated as the initial linear slope of the stress-strain curve before yield in dry samples. For wetted samples, the linear slope from 0 to 2.5% strain was used as no definitive yield point was seen. Toughness was calculated as the area under the stress-strain curves.

Additional samples were tested for supercontraction using the tensile tester and an environmental chamber as described by Boutry and Blackledge (2010). Across spider silks, higher proportions of proline-rich protein motifs are correlated with higher supercontraction (Liu et al. 2007; Boutry and Blackledge 2010; Marhabaie et al. 2014). Thus, we reasoned that high supercontraction would be indirect evidence in support of the proline-containing –GPGXX– amino acid motifs characteristic of flagelliform silk proteins (Hayashi and Lewis 1998). Cribellate threads were stretched to 15 μN and restrained as humidity was increased ~30 to <90% (RH) to measure changes in fiber tension, which was then converted to stress. The restrained fiber was then relaxed back to original tension when mounted to measure fiber shrinkage.

Statistical analysis

We used a general linear mixed model (test 1) to test between species averages and between treatments within species of mechanical properties of cribellate axial silk. The combinations of spider species and silk dry/wet treatments were considered as a fixed factor and coded as three dummy variables based on planned contrasts to estimate the difference between (1) wet *H. cavatus* and dry *H. cavatus*, (2) wet *U. plumipes* silk and dry *U. plumipes* silk, and (3) averages of *H. cavatus* and *U. plumipes* silk. Two random factors were used in the mixed model: (1) spider individual, to compare differences between treatments within individual, and (2) treatment within individual, to adjust for pseudo-replication within individual and within treatment. Parameters in mixed models were tested by using t value where the degrees of freedom were calculated using Welch-Satterthwaite equations. We also used a less conservative general linear model (test 2), which excluded all random factors. The standard errors of all parameters were adjusted by using the HC3 sandwich estimators to cope with heteroscedasticity among groups (Zeileis 2004). Sample size of treatments (N = spider individuals, n = silk samples): *H. cavatus* dry: $N = 7$, $n = 27$, *H. cavatus* wet: $N = 6$, $n = 23$, *U. plumipes* dry: $N = 3$, $n = 7$, and *U. plumipes* wet: $N = 3$, $n = 8$.

Results

We found that cribellate axial thread compliance and extensibility were affected by water. When tested in a wetted state (>90% RH), Young's modulus decreased ~7× in *H. cavatus* silk (Fig. 2c, Tables 1 and 2), and true strain at break increased by ~30% (Fig. 2b, Tables 1 and 2). We found that Young's modulus also decreased in *U. plumipes* silk by ~50% (Fig. 2c, Tables 1 and 2) when tested at high RH, though only test 2 provided a statistically significant difference, and true strain at break increased by ~20% (Fig. 2c, Tables 1 and 2), perhaps as a consequence of sample size. We did not find a significant effect of water on either true stress at break or toughness within species (Fig. 2a and d, Table 2). We found differences in true stress at break, Young's modulus, and toughness between species (Fig. 2, Table 2). Tests for supercontraction of cribellate axial silks revealed very low shrinkage and supercontraction stress values (Table 3).

Cribellate axial silk tested under dry conditions displayed mechanical behavior similar to that previously described by Blackledge and Hayashi (2006b). Cribellate silk threads tested in dry conditions displayed an initial elastic region where *H. cavatus* silk showed a pronounced yield point where the slope of the stress-strain decreased post-yield indicating a change in fiber stiffness (Fig. 3), which agrees with observations made by Blackledge and Hayashi (2006b). However, *U. plumipes* silk showed a less discernable yield point (Fig. 3). The initial elastic modulus of the two species we tested (Young's modulus: *H. cavatus*: 3.40 GPa, *U. plumipes*: 0.47 GPa) is within the range of the reported ~1-GPa value for other cribellate web-building spiders (Blackledge and Hayashi 2006a, Table 2). After yielding, silk threads became

Fig. 2 Mechanical properties of dry (~30% RH) and wetted (>90% RH) cribellate axial silk from two cribellate web-building spiders (mean ± SEM). Results of a two-way mixed model approach (test 1) are presented. *Horizontal lines* within or between species indicate differences. Significance levels from test 1 are indicated in *black above lines* where *** $p < 0.001$, ** $p < 0.01$, * $p < 0.05$, . $p < 0.10$, x NS. Significance levels from results of a one-way model (test 2) are presented in gray beneath lines (*See* Table 1 for mean and variance values)
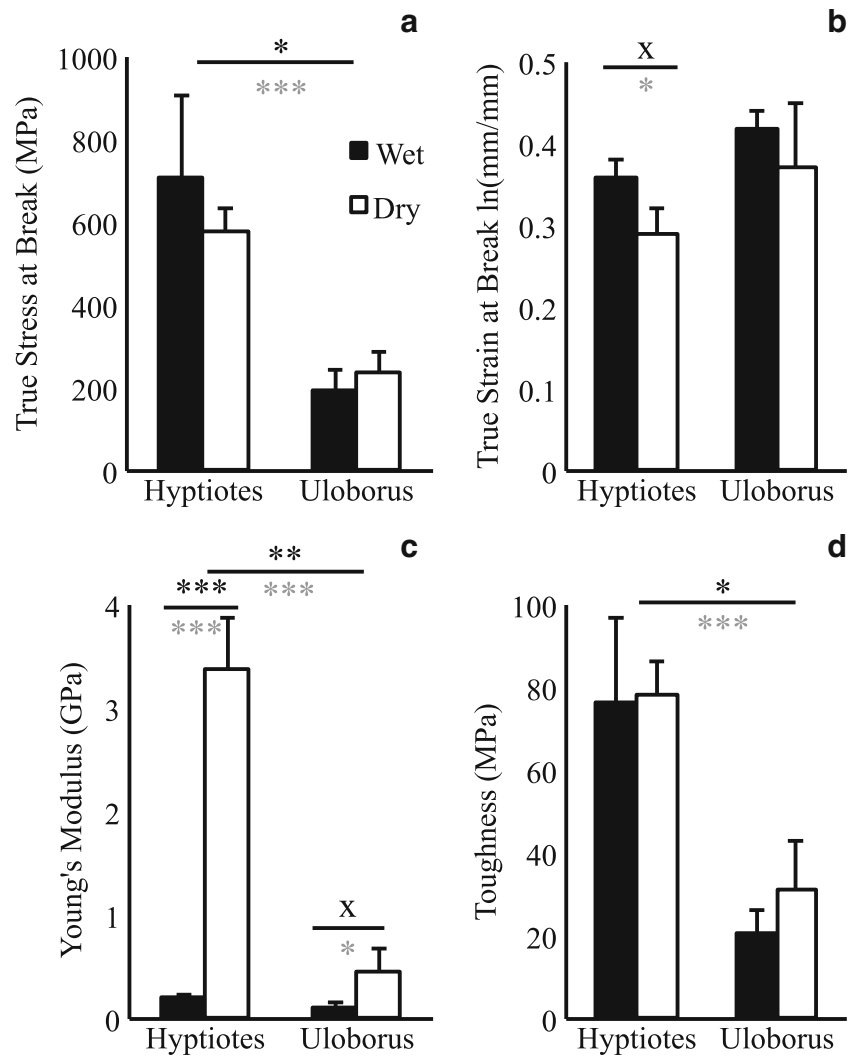
more compliant for up to ~20–25% strain before exhibiting strain-hardening that was characterized by a rapid increase in slope of the stress-strain curve before failure, as typical in other silk types (Blackledge and Hayashi 2006b, Fig. 3).

The mechanical behavior of cribellate axial silk tested in high RH displayed marked differences to silks tested in dry state for both spider species (Fig. 3). Young's modulus decreased significantly (Fig. 2c) and wetted fibers lacked a discernable yield point (Fig. 3 inset), in contrast to dry state fibers. Wetted fibers were compliant for a longer time, ~30–35% strain, before strain-hardening. This softening of the silk fiber by water is seen to a high degree (>100% strain) in flagelliform silk (Blackledge and Hayashi 2006b) but to a much lesser degree in major ampullate silk (30–60% strain) and minor ampullate silk (~10% strain, Guinea et al. 2012).

The shift in mechanical performance of cribellate axial silk between dry and wetted states is not as dramatic as the shift seen in flagelliform capture silk and is instead within the range exhibited by minor ampullate silk and major ampullate silk

(Table 2). Young's modulus decreased by a single order of magnitude when tested at high humidity (*H. cavatus* dry: 3.4 ± 0.48 GPa, wet: 0.2 ± 0.02 GPa, Table 2). In contrast, Young's modulus of naturally occurring flagelliform silk coated in aqueous, aggregate glue is extremely low (*A. trifasciata*: 0.008 GPa, Table 2) and studies that have experimentally dried these fibers by removing the aggregate glue revealed an increase in modulus by up to three orders of magnitude (*A. trifasciata*: ~5.5 GPa, Table 2). Like cribellate silk, both MiS and MAS silk show a high modulus in their natural, dry state of ~10 GPa, which decreases by only ~1 order of magnitude in MiS and 1–3 orders of magnitude in MAS (Table 2). Breaking strain of cribellate axial silk increased by ~20% when fibers were wetted which is more than five times smaller than the >100% increase in breaking strain for natural viscid fibers compared to a dry state, but similar to the ~15% difference between wetted and dried MiS (Table 2).

Supercontraction generated very little stress (10.18 ± 2.95 MPa, *H. cavatus*; 2.91 ± 1.52 MPa, *U. plumipes*) or macroscopic fiber

Table 1 Results from two statistical tests of differences in mechanical properties of cribellate silk between within-species treatments and species averages from two cribellate web-building spiders

Property[a]	Statistical test	Coefficient	Estimate	SE	df	t value	p[c]
True stress	Test 1	Intercept	427.26	80.725	9.05	5.29	**<0.001**
True stress	Test 1	*H. cavatus* silk (wet-dry)	123.81	152.95	9.29	0.81	0.438
True stress	Test 1	*U. plumipes* silk (wet-dry)	−35.71	227.64	8.55	−0.16	0.879
True stress	Test 1	*H. cavatus* (ave)-*U. plumipes* (ave)	−428	161.45	9.05	−2.65	**0.026**
True stress	Test 1	Random effect SD[c]:spider individual: 126.5, treatment:individual: 253.6					
True stress	Test 2	Intercept	405.88	28.83	60	14.08	**<0.001**
True stress	Test 2	*H. cavatus* silk (wet-dry)	77.74	106.32	60	0.73	0.467
True stress	Test 2	*U. plumipes* silk (wet-dry)	−15.71	44.68	60	−0.35	0.726
True stress	Test 2	*H. cavatus* (ave)-*U. plumipes* (ave)	−393.63	57.66	60	−6.83	**<0.001**
True strain	Test 1	Intercept	0.36	0.02	16.59	20.04	**<0.001**
True strain	Test 1	*H. cavatus* silk (wet-dry)	0.06	0.04	12.84	1.72	0.109
True strain	Test 1	*U. plumipes* silk (wet-dry)	0.08	0.06	18.36	1.26	0.223
True strain	Test 1	*H. cavatus* (ave)-*U. plumipes* (ave)	0.06	0.04	16.59	1.66	0.115
True strain	Test 1	Random effect SD:spider individual: <0.001, treatment:individual: 0.05					
True strain	Test 2	Intercept	0.35	0.01	60	23.69	**<0.001**
True strain	Test 2	*H. cavatus* silk (wet-dry)	0.06	0.03	60	2.19	**0.033**
True strain	Test 2	*U. plumipes* silk (wet-dry)	0.09	0.05	60	1.64	0.106
True strain	Test 2	*H. cavatus* (ave)-*U. plumipes* (ave)	0.06	0.03	60	1.85	0.070
Modulus	Test 1	Intercept	1.05	0.21	8.41	5.04	**<0.001**
Modulus	Test 1	*H. cavatus* silk (wet-dry)	−3.16	0.43	8.20	−7.33	**<0.001**
Modulus	Test 1	*U. plumipes* silk (wet-dry)	−0.39	0.68	8.47	−0.58	0.578
Modulus	Test 1	*H. cavatus* (ave)-*U. plumipes* (ave)	−1.47	0.42	8.41	−3.51	**0.007**
Modulus	Test 1	Random effect SD:spider individual: 0.18, treatment:individual: 0.66					
Modulus	Test 2	Intercept	1.06	0.10	60	11.16	**<0.001**
Modulus	Test 2	*H. cavatus* silk (wet-dry)	−3.10	0.30	60	−10.44	**<0.001**
Modulus	Test 2	*U. plumipes* silk (wet-dry)	−0.48	0.24	60	−2.00	**0.049**
Modulus	Test 2	*H. cavatus* (ave)-*U. plumipes* (ave)	−1.39	0.19	60	−7.27	**<0.001**
Toughness	Test 1	Intercept	51.01	8.56	17.11	5.96	**<0.001**
Toughness	Test 1	*H. cavatus* silk (wet-dry)	−2.81	18.47	14.73	−0.15	0.881
Toughness	Test 1	*U. plumipes* silk (wet-dry)	−8.43	28.83	18.24	−0.30	0.773
Toughness	Test 1	*H. cavatus* (ave)-*U. plumipes* (ave)	−51.62	17.12	17.11	−3.02	**0.008**
Toughness	Test 1	Random effect SD:spider individual:<0.001, treatment:individual: 29.38					
Toughness	Test 2	Intercept	49.14	3.74	60	13.14	**<0.001**
Toughness	Test 2	*H. cavatus* silk (wet-dry)	−7.29	13.35	60	−0.55	0.587
Toughness	Test 2	*U. plumipes* silk (wet-dry)	−5.64	6.75	60	−0.84	0.407
Toughness	Test 2	*H. cavatus* (ave)-*U. plumipes* (ave)	−49.45	7.48	60	−6.61	**<0.001**

[a] Units of measure: Young's modulus (GPa), toughness (MPa), true strain ln(mm/mm), true stress (MPa)

[b] Tests 1 and 2 refer to GLMM and GLM statistical methods used, respectively (*See* "Materials and methods" in text)

[c] Bold font indicates a significance level of $p < 0.05$

shrinkage (0.015 ± 0.005%, *H. cavatus*; 0.07 ± 0.03%, *U. plumipes*) in cribellate silk of two spiders (Table 3). A previous study by Liao et al. (2011) found that cribellate silk produced by *U. walckenaerius* generated, on average, 21 mN of force during

Table 2 Tensile properties[a] of silks used by ecribellate orb weaving and cribellate web-building spiders tested under various conditions

True values

Silk type	Spider	Testing conditions[b]	N spiders, n silk samples	Young's modulus (GPa)	Ultimate stress (MPa)	Ultimate strain ln(mm/mm)	Toughness (MPa)	Reference
Cribellate axial	Uloborus walkenaerius	20% RH	1, 1	–	–	~0.69	–	Liao et al. 2011[d]
Cribellate axial	Uloborus walkenaerius	60% RH	1, 1	–	–	~0.53	–	Liao et al. 2011[d]
Cribellate axial	Uloborus walkenaerius	90% RH	1, 1	–	–	~0.47	–	Liao et al. 2011[d]
Cribellate axial	Uloborus walkenaerius	99% RH	1, 1	–	–	~0.37	–	Liao et al. 2011[d]
Cribellate axial	Hyptiotes cavatus	~30% RH	7, 23	3.4 ± 0.48	577 ± 58	0.29 ± 0.03	78 ± 8	This study
Cribellate axial	Hyptiotes cavatus	>90% RH	6, 20	0.2 ± 0.02	709 ± 196	0.36 ± 0.02	77 ± 20	This study
Cribellate axial	Uloborus plumipes	~30% RH	3, 6	0.47 ± 0.21	237 ± 49	0.37 ± 0.08	31 ± 12	This study
Cribellate axial	Uloborus plumipes	~90% RH	3, 7	0.12 ± 0.05	194 ± 52	0.42 ± 0.02	21 ± 5	This study
Cribellate axial	Deinopis spinosa	Dry	5, 27	1.15 ± 0.31	404 ± 65	0.73 ± 0.14	92 ± 19	Blackledge and Hayashi 2006a
Cribellate axial	Hyptiotes cavatus	Dry	3, 22	7.04 ± 0.37	1439 ± 15	0.44 ± 0.04	206 ± 13	Blackledge and Hayashi 2006a
Cribellate axial	Hyptiotes gertschi	Dry	2, 24	1.06 ± 0.33	1171 ± 227	0.41 ± 0.04	120 ± 17	Blackledge and Hayashi 2006a
Cribellate axial	Uloborus diversus	Dry	11, 81	1.05 ± 0.33	1379 ± 105	0.32 ± 0.01	118 ± 11	Blackledge and Hayashi 2006a
Viscid	Araneus sericatus	Wet	–, 41		1270 ± 45	1.19 ± 0.05	150 ± 9	Denny 1976
Viscid	Araneus diadematus	Wet	–, 6		1338 ± 80	1.75 ± 0.15	283 ± 18	Köhler and Vollrath 1995
Viscid	Araneus diadematus	Wet	–, 4	0.012 ± 0.014	952 ± 447	1.36 ± 0.31	178 ± 71	Sensenig et al. 2010
Viscid	Araneus marmoreus	Wet	–, 5	0.005 ± 0.002	914 ± 315	1.45 ± 0.06	163 ± 64	Sensenig et al. 2010
Viscid	Araneus trifolium	Wet	–, 7	0.003 ± 0.001	1143 ± 169	1.72 ± 0.14	210 ± 45	Sensenig et al. 2010
Viscid	Argiope aurantia	Wet	–, 17	0.009 ± 0.011	1034 ± 344	1.57 ± 0.24	211 ± 99	Sensenig et al. 2010
Viscid	Argiope trifasciata	Wet	–, 9	0.008 ± 0.005	949 ± 292	1.44 ± 0.16	185 ± 65	Sensenig et al. 2010
Viscid	Gasteracantha cancriformis	Wet	–, 11	0.027 ± 0.018	986 ± 284	0.96 ± 0.10	145 ± 47	Sensenig et al. 2010
Viscid	Larinioides cornutus	Wet	–, 26	0.011 ± 0.008	1207 ± 377	1.27 ± 0.20	225 ± 84	Sensenig et al. 2010
Viscid	Leucauge venusta	Wet	–, 12	0.058 ± 0.046	887 ± 437	0.89 ± 0.14	148 ± 74	Sensenig et al. 2010
Viscid	Metepeira labyrinthea	Wet	–, 9	0.013 ± 0.019	778 ± 283	1.03 ± 0.11	123 ± 48	Sensenig et al. 2010
Viscid	Neoscona crucifera	Wet	–, 15	0.010 ± 0.005	1095 ± 384	1.48 ± 0.17	252 ± 99	Sensenig et al. 2010
Viscid	Neoscona domiciliorum	Wet	–, 4	0.020 ± 0.009	866 ± 233	1.13 ± 0.26	167 ± 67	Sensenig et al. 2010
Viscid	Nephila clavipes	Wet	–, 13	0.005 ± 0.007	231 ± 77	1.52 ± 0.23	39 ± 14	Sensenig et al. 2010
Viscid	Argiope argentata	Wet	5, 87	0.001 ± 0.0001	534 ± 40	1.72 ± 0.05	75 ± 6	Blackledge and Hayashi 2006b
Viscid	Argiope trifasciata	Cleaned[c]	–, 13	6 ± 4	800 ± 200	0.5 ± 0.2	–	Guinea et al. 2010
Viscid	Argiope trifasciata	Cleaned[c]	–, 4	5 ± 1	800 ± 100	0.76 ± 0.08	250 ± 50	Perea et al. 2013
Major ampullate	Araneus gemmoides	Dry	3, 23	8.3 ± 1	1376 ± 106	0.22 ± 0.03	141 ± 21	Swanson et al. 2006
Major ampullate	Argiope argentata	Dry	8, 59	13.5 ± 3.5	1463 ± 231	0.18 ± 0.02	116 ± 25	Swanson et al. 2006
Major ampullate	Gasteracantha cancriformis	Dry	3, 38	8.0 ± 2.1	1315 ± 338	0.30 ± 0.04	178 ± 45	Swanson et al. 2006
Major ampullate	Latrodectus hesperus	Dry	9, 70	10.2 ± 2.6	1469 ± 263	0.20 ± 0.05	151 ± 42	Swanson et al. 2006
Major ampullate	Leucauge venusta	Dry	6, 61	10.6 ± 2.3	1215 ± 233	0.17 ± 0.04	111 ± 31	Swanson et al. 2006
Major ampullate	Mastophora hutchinsoni	Dry	3, 21	9.4 ± 1.3	1137 ± 116	0.27 ± 0.05	140 ± 25	Swanson et al. 2006
Major ampullate	Metepeira grandiosa	Dry	10, 88	10.6 ± 4.4	1049 ± 373	0.24 ± 0.08	120 ± 65	Swanson et al. 2006
Major ampullate	Nephila clavipes	Dry	17, 66	13.8 ± 3.6	1441 ± 310	0.30 ± 0.06	181 ± 48	Swanson et al. 2006
Major ampullate	Deinopis spinosa	Dry	3, 24	13.5 ± 3.3	1329 ± 376	0.19 ± 0.03	136 ± 31	Swanson et al. 2006
Major ampullate	Uloborus diversus	Dry	7, 61	9.1 ± 2.4	1078 ± 310	0.23 ± 0.06	129 ± 39	Swanson et al. 2006
Major ampullate	Argiope trifasciata	35% RH	2, 3	10.7 ± 0.3	1300 ± 200	0.17 ± 0.02	90 ± 30	Guinea et al. 2012

Table 2 (continued)

True values

Silk type	Spider	Testing conditions[b]	N spiders, n silk samples	Young's modulus (GPa)	Ultimate stress (MPa)	Ultimate strain ln(mm/mm)	Toughness (MPa)	Reference
Major ampullate	Argiope trifasciata	In water	2, 3	0.022 ± 0.001	1420 ± 50	0.95 ± 0.03	185 ± 8	Guinea et al. 2012
Major ampullate	Nephila inaurata	35% RH	2, 3	14.2 ± 0.6	1800 ± 60	0.26 ± 0.01	264 ± 5	Guinea et al. 2012
Major ampullate	Nephila inaurata	In water	2, 3	0.041 ± 0.004	1700 ± 100	0.67 ± 0.01	280 ± 10	Guinea et al. 2012
Major ampullate	Araneus diadematus	25% RH	5, 25–50	7.8 ± 0.8	688 ± 44	0.10 ± 0.02	–	Shao et al. 1999[d]
Major ampullate	Araneus diadematus	In water	5, 25–50	~0.1	845 ± 65	0.26 ± 0.03	–	Shao et al. 1999[d]
Major ampullate	Argiope trifasciata	~15% RH	1, 2	~10	~1300	~0.26	–	Plaza et al. 2006
Major ampullate	Argiope trifasciata	~100% RH	1, 2	~0.03	~725	~1.06	–	Plaza et al. 2006
Minor ampullate	Argiope argentata	Dry	8, 51	10.6 ± 1.2	923 ± 154	0.33 ± 0.033	137 ± 22	Blackledge and Hayashi 2006b
Minor ampullate	Argiope trifasciata	Dry	–, 11	8.9 ± 0.5	~750	~0.44	150 ± 12	Hayashi et al. 2004
Minor ampullate	Nephila inaurata	35% RH	2, 3	11.2 ± 0.7	1500 ± 200	0.46 ± 0.05	300 ± 50	Guinea et al. 2012
Minor ampullate	Nephila inaurata	In water	2, 3	0.39 ± 0.03	1000 ± 100	0.53 ± 0.09	210 ± 60	Guinea et al. 2012
Minor ampullate	Argiope trifasciata	35% RH	2, 3	10 ± 0.4	1040 ± 60	0.45 ± 0.02	240 ± 20	Guinea et al. 2012
Minor ampullate	Argiope trifasciata	In water	2, 3	1.42 ± 0.09	1220 ± 200	0.51 ± 0.01	245 ± 25	Guinea et al. 2012

– data not available

[a] Values reported as mean ± SEM (SD for Sensenig et al. (2010)) or as (~) mean approximations reported from text and/or figures of reference

[b] Dry refers to untreated silk tested under ambient conditions (20–70% RH), wet refers to untreated viscid silk tested under ambient conditions

[c] Aggregate glue coating removed via centrifugation

[d] True values calculated from original engineering values

Table 3   Supercontraction properties[a] of various silks used by spiders

Silk type	Species	Supercontration stress (MPa)	Shrinkage (%)	Reference
Cribellate	*Uloborus plumipes*	10.18 ± 2.95	0.015 ± 0.005	This study
Cribellate	*Hyptiotes cavatus*	2.91 ± 1.52	0.07 ± 0.03	This study
Flagelliform	*Argiope trifasciata*	–	32	Guinea et al. 2010
Major ampullate	Orb web spiders (eight species)	75 ± 11	40 ± 6	Boutry and Blackledge 2010
Major ampullate	Non–Orb web spiders (20 species)	41 ± 8	7.5 ± 2	Boutry and Blackledge 2010
Major ampullate	*Nephila clavipes*	100	–	Blackledge et al. 2009a, b)
Major ampullate	*Nephila clavipes*	–	5 ± 2	Jelinski et al. 1999
Minor ampullate	*Nephila inaurata*	–	5.6 ± 0.3	Guinea et al. 2012
Minor ampullate	*Argiope trifasciata*	–	2.8 ± 0.7	Guinea et al. 2012

Values reported as mean ± SEM. – data not available

supercontraction, which was much higher than what we observed (Table 3). Methodological differences in exposure times of silk to humidity during testing (1–2 vs. 15 min) and potential effects of between species differences may account for the discrepancy between studies. Moreover, even slight changes in pretensioning of

fibers dramatically influence the amount of force generated during supercontraction (Boutry and Blackledge 2010).

Discussion

Our study tests the hypothesis that a key protein explaining viscid capture silk mechanics may be present in ancestral cribellate axial fibers, but that its effects are masked by the dry nature of the cribellate adhesive. We compare the effects of water on the mechanical properties of cribellate silk to viscid silk and also to the major ampullate silk that forms the dry structural threads in both cribellate and ecribellate orb webs. We found that wetted cribellate silk became more compliant and extensible, but only to a magnitude similar to web structural silks like minor ampullate silk and major ampullate of some orb web species rather than viscid capture silk (Fig. 2, Tables 1 and 2). We also observed very little supercontraction when cribellate axial fibers were exposed to increased humidity, again dissimilar to viscid capture silk (Table 3). These results do not fit the prediction that flagelliform proteins are expressed at a high-enough level in cribellate silk to influence its material properties and therefore do not support the hypothesis that flagelliform silk's mechanical performance evolved as an exaptation. Instead, our data supports the hypothesis of a punctuated change in mechanical properties during the origin of viscid silk.

Supercontraction and proline are strongly correlated in several silk types (Liu et al. 2007; Boutry and Blackledge 2010; Marhabaie et al. 2014) as proline tends to induce β-turn and β-spiral structures and is hypothesized to inhibit crystalline formation (Jelinski 1998; Creager et al. 2010; Jenkins et al. 2010). High levels of proline from repetitive –GPGXX– motifs are a hallmark of flagelliform silk proteins (Hayashi and Lewis 1998) and explain the high extensibility of viscid silk when it is covered with aqueous glue. The weak supercontraction we found for cribellate axial silk (Table 3)
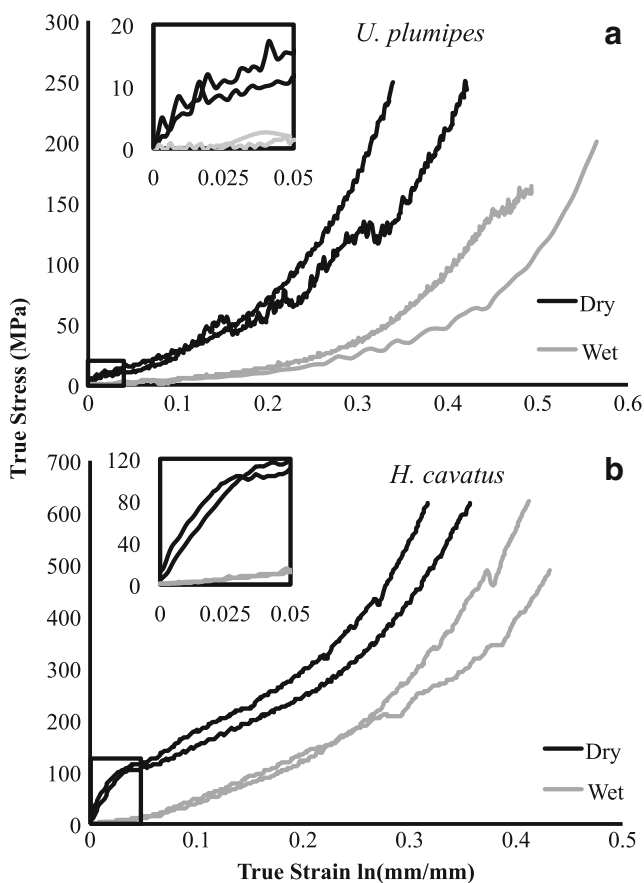

Fig. 3 Qualitative comparison of mechanical performance between cribellate axial silk threads in dry state (~30% RH) and wet state (>90% RH). Two representative curves per treatment from two cribellate web-building spider species are shown. Inset highlights initial slopes of curves up to 5% strain

suggests that either flagelliform-like fibroins are expressed at low levels or some other aspect of molecular structure inhibits the mobility and modulation of the proline-rich, β-turn nanosprings (e.g., such as β-sheet nanocrystals). This could explain why we did not observe much similarity of response to water of cribellate axial silk to proline-rich viscid silk, but did find similarity to more proline-poor silks, such as minor ampullate silk and major ampullate silk from certain species. For example, MiS from multiple taxa including *Argiope argentata*, *Araneus diadematus*, and *Neoscona ravilla* (Work and Young 1987; Colgin and Lewis 1998) is composed of less than 1% proline, whereas, MAS from *Nephila* spiders, including *Nephila clavipes* (Work and Young 1987; Lombardi and Kaplan 1990), *Nephila edulis*, and *Nephila senegalensis* (Liu et al. 2007) is composed of less than 6% proline. Furthermore, direct measurement of amino acid composition of cribellate axial fibers is needed to confirm proline concentration and to make useful comparison to other silk types.

We show that there is little similarity in performance of the wetted state of cribellate axial silk to the characteristically high extensibility and compliance of wet viscid silk. This makes a gradual transition in mechanics of axial threads from stiff cribellate threads to compliant flagelliform threads unlikely. Our data suggest the unique extensibility and compliance of the axial core fiber of viscid capture silk likely evolved rapidly during the origin of viscid adhesive silk itself (Köhler and Vollrath 1995; Blackledge and Hayashi 2006a), rather than in a cribellate ancestor. Thus, how the transition from cribellate silk to viscid silk occurred still remains an open question that needs further exploration.

References

Amarpuri G, Zhang C, Diaz C, Opell BD, Blackledge TA, Dhinojwala A (2015) Spiders tune glue viscosity to maximize adhesion. ACS Nano 9(11):11472–11478

Blackledge TA, Hayashi CY (2006a) Unraveling the mechanical properties of composite silk threads spun by cribellate orb-weaving spiders. J Exper Biol 209:3131–3140

Blackledge TA, Hayashi CY (2006b) Silken toolkits: biomechanics of silk fibers spun by the orb web spider *Argiope argentata* (Fabricius 1775). J Exper Biol 209(13):2452–2461

Blackledge TA, Cardullo RA, Hayashi CY (2005) Polarized light microscopy, variability in spider silk diameters and the mechanical characterization of spider silk. Invert Biol 124(2):165–173

Blackledge TA, Scharff N, Coddington JA, Szüts T, Wenzel JW, Hayashi CY, Agnarsson I (2009a) Reconstructing web evolution and spider diversification in the molecular era. Proc National Acad Sci 106(13): 5229–5234

Blackledge TA, Boutry C, Wong SC, Baji A, Dhinojwala A, Sahni V, Agnarsson I (2009b) How super is supercontraction? Persistent versus cyclic responses to humidity in spider dragline silk. J Exper Biol 212(13):1981–1989

Blackledge TA, Kuntner M, Agnarsson I (2011) The form and function of spider orb webs: evolution from silk to ecosystems. Adv Insect Phys 41:175

Bond JE, Opell BD (1998) Testing adaptive radiation and key innovation hypotheses in spiders. Evolution:403–414

Bond JE, Garrison NL, Hamilton CA, Godwin RL, Hedin M, Agnarsson I (2014) Phylogenomics resolves a spider backbone phylogeny and rejects a prevailing paradigm for orb web evolution. Curr Biol 24: 1765–1771

Bott RA, Baumgartner W, Bräunig P, Menzel F, Joel AC (2017) Adhesion enhancement of cribellate capture threads by epicuticular waxes of the insect prey sheds new light on spider web evolution. Proc R Soc B 284(1855):20170363

Boutry C, Blackledge TA (2010) Evolution of supercontraction in spider silk: structure-function relationship from tarantulas to orb-weavers. J Exper Biol 213(20):3505–3514

Boutry C, Řezáč M, Blackledge TA (2011) Plasticity in major ampullate silk production in relation to spider phylogeny and ecology. PLoS One 6(7):e22467

Coddington JA (1982) Monophyletic origin of orb-webs. Amer Zool 22(4):886–886

Coddington JA (1986) The monophyletic origin of the orb web. In: Shear WA (ed) spiders: webs, behavior, and evolution, 319-63. Stanford University Press, Stanford

Coddington JA (1990) Cladistics and spider classification: araneomorph phylogeny and the monophyly of orbweavers (Araneae: Araneomorphae; Orbiculariae). Acta Zool Fenn 190(190):75–87

Coddington JA, Levi HW. (1991) Systematics and evolution of spiders (Araneae). Annu Rev Ecol Syst (1):565–92

Colgin MA, Lewis RV (1998) Spider minor ampullate silk proteins contain new repetitive sequences and highly conserved non-silk-like "spacer regions". Protein Sci 7(3):667–672

Creager MS, Jenkins JE, Thagard-Yeaman LA, Brooks AE, Jones JA, Lewis RV, Holland GP, Yarger JL (2010) Solid-state NMR comparison of various spiders' dragline silk fiber. Biomacromolecules 11(8):2039

Denny M (1976) The physical properties of spider's silk and their role in the design of orb-webs. J Exper Biol 65(2):483–506

Dimitrov D, Lopardo L, Giribet G, Arnedo MA, Álvarez-Padilla F, Hormiga G (2011) Tangled in a sparse spider web: single origin of orb weavers and their spinning work unravelled by denser taxonomic sampling. Proc R Soc B 279:1341–1350

Eberhard WG (1982) Behavioral characters for the higher classification of orb-weaving spiders. Evolution 1067–95

Eberhard WG (1990) Function and phylogeny of spider webs. Annu Rev Ecol Syst 21(1):341–372

Eberhard WG, Barrantes G (2015) Cues guiding uloborid construction behavior support orb web monophyly. J Arachnol 43(3):371–387

Eles PT, Michal CA (2004) Strain dependent local phase transitions observed during controlled supercontraction reveal mechanisms in spider silk. Macromolecules 37(4):1342–1345

Elettro H, Neukirch S, Antkowiak A, Vollrath F (2015) Adhesion of dry and wet electrostatic capture silk of uloborid spider. Sci Nat (7–8):1–4

Fernandez R, Hormiga G, Giribet G (2014) Phylogenomic analysis of spiders reveals nonmonophyly of orb weavers. Curr Biol 24:1772–1777

Foelix R (2011) Biology of spiders, 3rd edn. Oxford Univ. Press, Oxford

Garb JE, DiMauro T, Vo V, Hayashi CY (2006) Silk genes support the single origin of orb webs. Science 312(5781):1762

Garrison NL, Rodriguez J, Agnarsson I, Coddington JA, Griswold CE, Hamilton CA, Hedin M, Kocot KM, Ledford JM, Bond JE (2016) Spider phylogenomics: untangling the Spider Tree of Life. PeerJ 4: e1719

Gatesy J, Hayashi C, Motriuk D, Woods J, Lewis R (2001) Extreme diversity, conservation, and convergence of spider silk fibroin sequences. Science 291(5513):2603–2605

Gosline JM, Denny MV, Demont ME (1984) Spider silk as rubber. Nature 309:551–552

Gould SJ, Vrba ES (1982) Exaptation—a missing term in the science of form. Paleobiology 8(1):4–15

Griswold CE, Coddington JA, Platnick NI, Forster RR (1999) Towards a phylogeny of entelegyne spiders (Araneae, Araneomorphae, Entelegynae). J Arachnol 53–63

Griswold CE, Ramírez MJ, Coddington JA, Platnick NI (2005) Atlas of phylogenetic data for entelegyne spiders (Araneae: araneomorphae: Entelegynae), with comments on their phylogeny. Proc Cal Acad Sci 56:1–324

Guinea GV, Pérez-Rigueiro J, Plaza GR, Elices M (2006) Volume constancy during stretching of spider silk. Biomacromolecules 7(7): 2173–2177

Guinea GV, Cerdeira M, Plaza GR, Elices M, Pérez-Rigueiro J (2010) Recovery in viscid line fibers. Biomacromolecules 11(5):1174–1179

Guinea GV, Elices M, Plaza GR, Perea GB, Daza R, Riekel C, Agulló-Rueda F, Hayashi C, Zhao Y, Perez-Rigueiro J (2012) Minor ampullate silks from Nephila and Argiope spiders: tensile properties and microstructural characterization. Biomacromolecules 13(7): 2087–2098

Hawthorn AC, Opell BD (2002) Evolution of adhesive mechanisms, in cribellar spider prey capture thread: evidence for van der Waals and hygroscopic forces. Biol J Linn Soc Lond 77:1–8

Hawthorn AC, Opell BD (2003) van der Waals and hygroscopic forces of adhesion generated by spider capture threads. J Exper Biol 206: 3905–3911

Hayashi CY, Lewis RV (1998) Evidence from flagelliform silk cDNA for the structural basis of elasticity and modular nature of spider silks. J Mol Biol 275(5):773–784

Hayashi CY, Lewis RV (2000) Molecular architecture and evolution of a modular spider silk protein gene. Science 287(5457):1477–1479

Hayashi CY, Blackledge TA, Lewis RV (2004) Molecular and mechanical characterization of aciniform silk: uniformity of iterated sequence modules in a novel member of the spider silk fibroin gene family. Mol Biol Evol 21(10):1950–1959

Jelinski LW (1998) Establishing the relationship between structure and mechanical function in silks. Curr Opinion Solid State Mater Sci 3(3):237–245

Jelinski LW, Blye A, Liivak O, Michal C, LaVerde G, Seidel A, Shah N, Yang Z (1999) Orientation, structure, wet-spinning, and molecular basis for supercontraction of spider dragline silk. Int J Biol Macromol 24(2):197–201

Jenkins JE, Creager MS, Butler EB, Lewis RV, Yarger JL, Holland GP (2010) Solid-state NMR evidence for elastin-like β-turn structure in spider dragline silk. Chem Commun 46(36):6714–6716

Joel AC, Kappel P, Adamova H, Baumgartner W, Scholz I (2015) Cribellate thread production in spiders: complex processing of nano-fibres into a functional capture thread. Arthropod Struct Dev 44(6):568–573

Köhler T, Vollrath F (1995) Thread biomechanics in the two orb-weaving spiders Araneus diadematus (Araneae, Araneidae) and Uloborus walckenaerius (Araneae, Uloboridae). J Exper Zool 271(1):1–7

Kullmann EJ (1972) The convergent development of orb-webs in cribellate and ecribellate spiders. Am Zool 12(3):395–405

Liao X, Yin G, Huang Z, Yao Y, Gu J, Han D (2011) Supercontraction on cribellate spider spiral silk with wet-rebuilt micro-structure. Mater Sci Eng C 31(2):128–133

Liu Y, Sponner A, Porter D, Vollrath F (2007) Proline and processing of spider silks. Biomacromolecules 9(1):116–121

Liu Y, Shao ZZ, Vollrath F (2008) Elasticity of spider silks. Biomacromolecules 9:1782–1786

Lombardi SJ, Kaplan DL (1990) The amino acid composition of major ampullate gland silk (dragline) of Nephila clavipes (Araneae, Tetragnathidae). J Arachnol 297–306

Marhabaie M, Leeper TC, Blackledge TA (2014) Protein composition correlates with the mechanical properties of spider (Argiope trifasciata) dragline silk. Biomacromolecules 15:20–29

Opell BD (1994) Factors governing the stickiness of cribellar prey capture threads in the spider family Uloboridae. J Morph 221:111–119

Opell BD (1997) The material cost and stickiness of capture threads and the evolution of orb-weaving spiders. Biol J Linn Soc 62(3):443–458

Opell BD (1999) Redesigning spider webs: stickiness, capture area, and the evolution of modern orb-webs. Evolutionary Ecol Res 1:503–516

Opell BD, Bond JE (2000) Capture thread extensibility of orb-weaving spiders: testing punctuated and associative explanations of character evolution. Biol J Linn Soc 70(1):107–120

Opell BD, Bond JE (2001) Changes in the mechanical properties of capture threads and the evolution of modern orb-weaving spiders. Evol Ecol Res 3(5):507–519

Opell BD, Hendricks ML (2007) Adhesive recruitment by the viscous capture threads of araneoid orb-weaving spiders. J Exper Biol 210: 553–560

Opell BD, Schwend HS (2009) Adhesive efficiency of spider prey capture threads. Zoology 112(1):16–26

Opell BD, Karinshak SE, Sigler MA (2011a) Humidity affects the extensibility of an orb-weaving spider's viscous thread droplets. J Exper Biol 214(17):2988–2993

Opell BD, Tran AM, Karinshak SE (2011b) Adhesive compatibility of cribellar and viscous prey capture threads and its implication for the evolution of orb-weaving spiders. J Exper Zool Part A: Ecol Genet Phys 315(6):376–384

Perea GB, Riekel C, Guinea GV, Madurga R, Daza R, Burghammer M, Hayashi C, Elices M, Plaza GR, Pérez-Rigueiro J. (2013) Identification and dynamics of polyglycine II nanocrystals in Argiope trifasciata flagelliform silk. Sci Rep 3. doi: 10.1038/srep03061

Pérez-Rigueiro J, Elices M, Plaza G, Real JI, Guinea GV (2005) The effect of spinning forces on spider silk properties. J Exper Biol 208(14):2633–2639

Peters HM (1987) Fine structure and function of capture threads. In: Ecophysiology of spiders, 187–202. Springer Berlin Heidelberg

Plaza GR, Guinea GV, Pérez-Rigueiro J, Elices M (2006) Thermo-hygro-mechanical behavior of spider dragline silk: glassy and rubbery states. J Polymer Sci B: Polymer Phys 44(6):994–999

Sahni, V, Blackledge TA, Dhinojwala A (2010) Viscoelastic solids explain spider web stickiness. Nat Commun 1. doi: 10.1038/ncomms1019

Savage KN, Gosline JM (2008) The role of proline in the elastic mechanism of hydrated spider silks. J Exper Biol 211(12):1948–1957

Sensenig A, Agnarsson I, Blackledge TA (2010) Behavioural and biomaterial coevolution in spider orb webs. J Evol Biol 23(9):1839–1856

Shao Z, Young RJ, Vollrath F (1999) The effect of solvents on spider silk studied by mechanical testing and single-fibre Raman spectroscopy. Int J Biol Macromol 24(2):295–300

Swanson BO, Blackledge TA, Beltrán J, Hayashi CY (2006) Variation in the material properties of spider dragline silk across species. Appl Phys A 82(2):213–218

Swanson BO, Blackledge TA, Hayashi CY (2007) Spider capture silk: performance implications of variation in an exceptional biomaterial. J Exper Zool A Ecol Genet Physiol 307:654–666

Termonia Y (1994) Molecular modeling of spider silk elasticity. Macromolecules 27(25):7378–7381

Vollrath F, Edmonds D (1989) Modulation of the mechanical properties of spider silk by coating with water. Nature 340:305–307

Work RW (1976) The force-elongation behavior of web fibers and silks forcibly obtained from orb-web-spinning spiders. Text Res J 46(7): 485–492

Work RW, Young CT (1987) The amino acid compositions of major and minor ampullate silks of certain orb-web-building spiders (Araneae, Araneidae). J Arachnol 65–80

Yang Z, Liivak O, Seidel A, LaVerde G, Zax DB, Jelinski LW (2000) Supercontraction and backbone dynamics in spider silk: 13C and 2H NMR studies. J Amer Chem Soc 122(37):9019–9025

Zeileis A (2004) Econometric computing with HC and HAC covariance matrix estimators. J Stat Softw 11(10):1–17 URL: http://www.jstatsoft.org/v11/i10/

Zschokke S, Vollrath F (1995) Unfreezing the behaviour of two orb spiders. Phys Behav 58(6):1167–1173